Electronic Supplementary Material (ESI) for Physical Chemistry Chemical Physics.

Supporting Information

On the coupling mechanism occurring at the neuron-nanoparticle interface

Greta Chiaravalli[1,2], Jasnoor[3,4], Tiziana Ravasenga[3,4], Elisabetta Colombo[3,4], Simona Francia[3,4], Stefano Di Marco[3,4], Riccardo Sacco[5], Grazia Pertile[6], Fabio Benfenati[3,4], Guglielmo Lanzani[1,2]

[1] Center for Nano Science Technology, Istituto Italiano di Tecnologia, Milano, Italy;
[2] Politecnico di Milano, Physics Department, Milano, Italy;
[3] Center for Synaptic Neuroscience and Technology, Istituto Italiano di Tecnologia, Genova, Italy;
[4] IRCCS Ospedale Policlinico San Martino, Genova, Italy
[5] Politecnico di Milano, Mathematics Department, Milano, Italy;
[6] Department of Ophthalmology, IRCCS Sacrocuore Don Calabria Hospital, Negrar, Verona, Italy.

The complete bio-hybrid model

The model accounts for:

- a time dependence to account for the light switching on/off effect on the NP polarization and also production of O_2^-;
- the drift and diffusion of the electrolytic ions Sodium, Potassium and Chlorine, present in the extracellular solution;
- a detailed description of the cleft region, accounting for the volume-filling effect induced by the adhesion protein;
- the interaction between neuron and the external environment through the Goldman-Hodgkin-Katz model of ion conductances.

The goal is to quantitatively give an estimation of the electrostatic perturbation exerted by the NP on the surrounding environment and to evaluate the concentration of superoxide reaching the neuron membrane, thus possibly triggering a chemical effect onto the cellular membrane.

The mathematical model

In the present model we couple the Drift-Diffusion model describing the P3HT nanoparticle (similar to what has been done in [3; 6]) with the multi-physical description of the electrolytic solution. In addition, we introduce an original formulation of the Poisson-Nernst-Planck model in the cleft proteinic region, in which we modify the electrochemical transport by adding a term proportional to the protein spatial distribution. This term describes the effect exerted on ions by proteins when they fill a certain volume space, thus staving off the ions which are repelled from the protein-filled region. The electro-diffusive motion of ions in the bulk electrolytic solution instead faithfully relate to the classical Poisson-Nernst-Planck model. In addition, we also include the modeling of the possible electrostatic and ionic interactions occurring with a neuronal cell positioned at the endpoint of the domain.

A drawing of the full system is reported in fig. 1: in panel A we show the schematic drawing of the full multi-physical and three-dimensional domain of a P3HT-NP engulfed into a neuron; in panel B instead we illustrate the mathematical computational domain under consideration.

Spatial domain

Equations are solved along a 1D system, reported in panel B of fig. 1. The one dimensional domain open interval $(0, W)$ comprises four subdomains, $\Omega = \{\Omega_1, \Omega_2, \Omega_2^{bis}, \Omega_3\}$, where Ω_1 represents the cleft region in between the neuron and the NP, Ω_2 the NP domain, Ω_2^{bis} the interstitial path which connects the extracellular region with the cleft environment and Ω_3 the extracellular electrolytic solution. The interface between the neuron and the cleft is located at $x = 0$, between P3HT-NP and the cleft is located at $x = R_1$ whereas the interface between the P3HT-NP and the electrolytic solution is located at $x = R_2$.

The ionic interstitial path, Ω_2^{bis}, also connects the points $x = R_1$ and $x = R_2$ accounting for a possible trajectory of the ions dispersed in solution.This may be physically supported by diffusive fluxes at both nodes R_1 and R_2 which may branch towards either the cleft or the extracellular medium depending on the physical environment. Without the description of

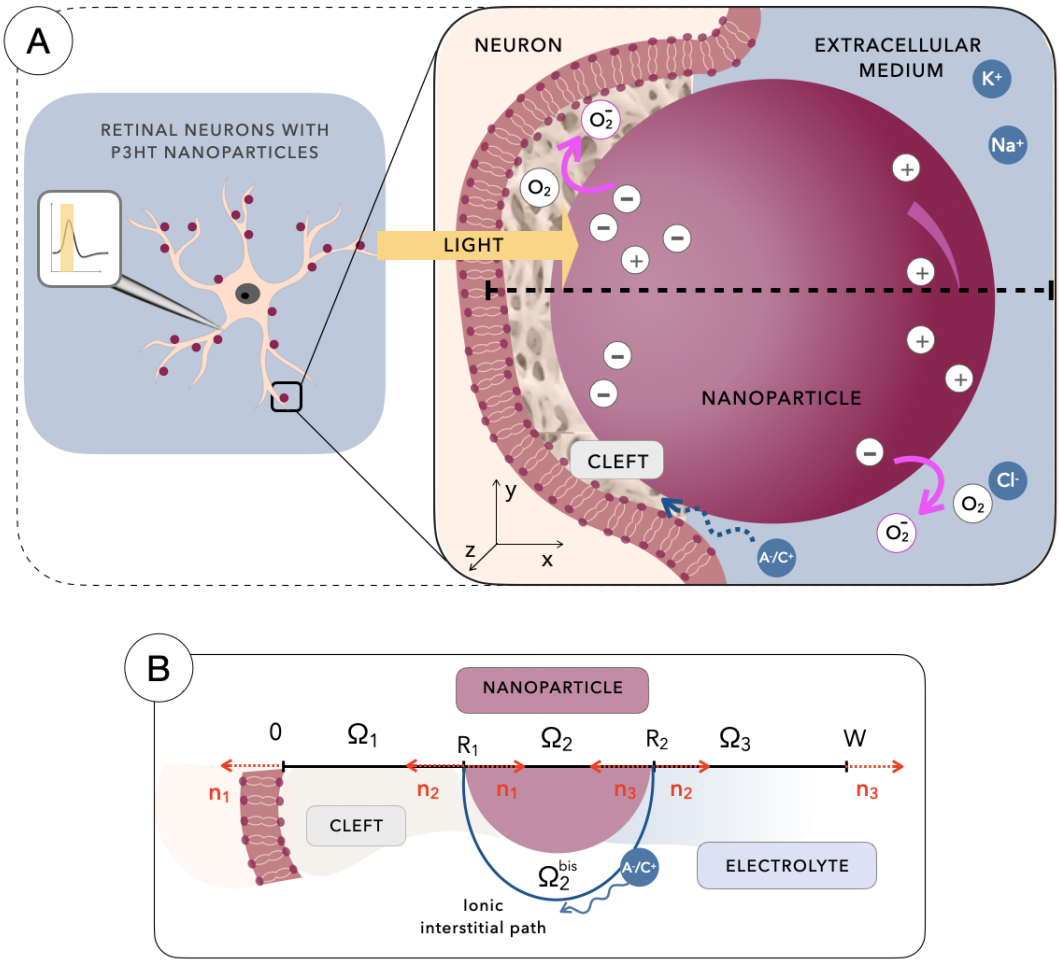

Figure 1: In the figure we show how we have translated the multi-physical domain of one of the many P3HT-NPs attached to the neuron membrane (as experimentally done in Maya-Vetencourt et al. [12, 11] and Francia et al. [6]) into a geometrical 1D representation of the system. In panel A we graphically represent a neuron, whose dendrites are covered by NPs (tens or hundred experimentally). If we zoom on one of this NP, we understand the more microscopic nature of the system: the NP is engulfed into the neuron membrane. However, a direct contact is hindered by the presence of a region called "cleft", an interstitial space supposedly filled by adhesion protein which allow the anchoring of the NP to the membrane. The symmetry of this complex system along the x axis reported in panel A allows us to model it with a 1D description, along the axis crossing the center of the NP. In panel B we report the geometrical domain adopted for the simulations, comprising the cleft, the NP and the extracellular region.

a possible connection between the cleft and the extracellular environment the two regions would be completely independent one from each other and the model would lose generality.

The nanoparticle diameter is assumed equal to 300 nm. The cleft region is instead modeled with a thickness of 30 nm and W is placed at 1330 nm. We also denote by $\mathbf{n}_1$, $\mathbf{n}_2$ and $\mathbf{n}_3$ the outward unit normal vectors associated with the three subdomains $\Omega_1, \Omega_2, \Omega_3$, respectively.

Temporal domain

The model equations are solved in the time domain $I_T := (0, T)$, where $T = 1$ s. Inside this time domain, to simulate a retinal physiological input, we define the light on interval as $I_T^{light} = (T_i, T_f)$, with $T_i = 0.1$ s and $T_f = 0.2$ s, represented in **??**. The light stimulus has a duration of 100 ms, unless differently specified.

The initial condition

In order to solve our system we require to know the initial condition of the system, which we supposed to be in a dark condition.

- As far as it regards all the ions, they are initialized across the whole domain of definition Ω_1, Ω_2^{bis} and Ω_3 as constant, with value equal to their electrolytic equilibrium concentration:

$$c_\alpha(x, 0) = c_\alpha^{bulk} \qquad \forall x \in \Omega_1 \cup \Omega_2^{bis} \cup \Omega_3 \tag{1}$$

$$c_{O_2^-}(x, 0) = c_{O_2^-}^{eq} \qquad \forall x \in \Omega_1 \cup \Omega_2^{bis} \cup \Omega_3 \tag{2}$$

- Concerning electrons and holes, they are initialized to the intrinsic concentration of the material in dark, $n_i = 10^{12}$ m^{-3}

$$p(x, 0) = n_i \qquad \forall x \in \Omega_2 \tag{3}$$

$$n(x, 0) = n_i \qquad \forall x \in \Omega_2 \tag{4}$$

- The initial electric potential is instead determined by solving the linear Poisson equation, interface and boundary conditions described in the following, assuming a $\rho^0 = 0$.

- With this set of initial conditions, we solve the steady state version of the model reported in the following sections in a dark condition and adopt the output dark steady state solutions as initial conditions of the time dependent model.

The modified Poisson-Nernst-Planck model

Given a 3-dimensional set of coordinates, indicated with $\underline{\mathbf{x}}$, it is well known that the equation describing the flux density of a charged mixture of ions α, can be derived from the momentum balance equation, and written as:

$$\mathbf{j}_\alpha = c_\alpha \mathbf{v}_\alpha \tag{5}$$

where $\mathbf{v}_\alpha$ represents the velocity of the ions, which can be related to several mechanisms. In particular the most common contributions in literature are those related to diffusional or electric gradient and to the drift induced by the fluid velocity in which the charged particle mixture is immersed. The three contributions read as follows:

* the convective flux density due to the drifting effect of the electric field on the charged particles

$$\mathbf{j}_\alpha^{\text{el}} = \mu_\alpha \frac{z_\alpha}{|z_\alpha|} c_\alpha \mathbf{E} \tag{6}$$

where the electric field $\mathbf{E} = -\nabla_{\underline{x}} \psi$;

* the diffusive flux density due to the molecular ion diffusion process described by Fick's law

$$\mathbf{j}_\alpha^{\text{diff}} = -D_\alpha \nabla_{\underline{x}} c_\alpha; \tag{7}$$

* the convective flux density due to the drifting effect of the velocity of the fluid component on the charged particles

$$\mathbf{j}_\alpha^{\text{fluid}} = c_\alpha \mathbf{v}_f; \tag{8}$$

Whereas the first two contributions are expected to exert a non negligible electro-diffusion effect in our system, we reasonably assume the extracellular medium in which the neuron and the NP are immersed to be still, particularly in the cleft interstitial region where, due to the reduced thickness, we do not expect any significant fluid velocity. Coherently, we neglect the fluid-velocity contribution of eq. (8).

However, we introduce an original modification to the model, accounting for a velocity of the ions induced by the protein filling a certain volume: due to the occupation of space caused by the volumetric presence of adhesion proteins, ions are repelled and tend to move towards more empty spaces. This contribution does not depend on the charge sign of the carrier, but solely on the concentration gradient of the protein: depending on how much protein fills the volume, ions drift away towards protein-free regions. We will refer to this drift term in the following as the **proteinic drift**.

$$\mathbf{j}_\alpha^{\text{p}} = -\mu_\alpha \mathrm{V_{th}} \frac{c_\alpha}{c_{\text{p}}} \nabla_{\underline{x}} c_{\text{p}}; \tag{9}$$

where c_{p} is the protein concentration. The ionic flux density in our model can be therefore written as:

$$\mathbf{j}_\alpha = -\mu_\alpha \frac{z_\alpha}{|z_\alpha|} c_\alpha \left(+\nabla_{\underline{x}} \psi + \frac{\mathrm{V_{th}}}{z_\alpha} \frac{\nabla_{\underline{x}} c_\alpha}{c_\alpha} + \frac{|z_\alpha| \mathrm{V_{th}}}{z_\alpha} \frac{\nabla_{\underline{x}} c_{\text{p}}}{c_{\text{p}}} \right) \tag{10}$$

One interpretation of the classical drift-diffusion transport model amounts to writing $\mathbf{j}_\alpha$ as a function of the gradient of a unified potential field, the electrochemical potential φ^{ec} which accounts for both the diffusive and the electrical contributions. We can define in our modified version of the Poisson-Nernst-Planck model, the electrochemical-proteinic potential φ_α^{ecp} as:

$$\varphi_\alpha^{\text{ecp}} = \varphi_\alpha^{\text{ec}} + \varphi_\alpha^{\text{p}} = \psi + \frac{\mathrm{V_{th}}}{z_\alpha} \ln \left(\frac{c_\alpha}{c_\alpha^{\text{ref}}} \right) + \frac{|z_\alpha| \mathrm{V_{th}}}{z_\alpha} \ln \left(\frac{c_{\text{p}}}{c_{\text{p}}^{\text{ref}}} \right) \tag{11}$$

being $\varphi_\alpha^{\text{p}}$ the proteinic potential for the ion α:

$$\varphi_\alpha^{\text{p}} = \frac{|z_\alpha| \mathrm{V_{th}}}{z_\alpha} \ln \left(\frac{c_{\text{p}}}{c_{\text{p}}^{\text{ref}}} \right) \tag{12}$$

Therefore, the flux density can be rewritten as:

$$\mathbf{j}_\alpha = -\mu_\alpha \frac{z_\alpha}{|z_\alpha|} c_\alpha \nabla_{\underline{x}} \varphi^{\text{ecp}} \tag{13}$$

The ions of the electrolytic solution

In the present model we solve the continuity equation for the three ions α, with α =Na^+, Cl^- and K^+ along the ionic path, constituted by the continuum of the three domains $\Omega_\alpha = \{\Omega_1 \cup \Omega_2^{\text{bis}} \cup \Omega_3\}$. A non trivial modification is performed on the Poisson-Nernst-Planck model for the ionic transport to account for the presence of the proteinic cleft region, which occupies the available volume in the interstitial region, inducing a repulsive current of ions which flow towards the free volume regions, as reported in the previouos paragraph. Based on the modified Poisson-Nernst-Planck model, we can write the continuity equation for the electrolytic ions α as:

$$\begin{cases} \dfrac{\partial c_\alpha}{\partial t} + \nabla_x \cdot \mathbf{j}_\alpha = 0 & \forall (x,t) \in (\Omega_\alpha \times I_T) \\ \mathbf{j}_\alpha = -\mu_\alpha \dfrac{z_\alpha}{|z_\alpha|} c_\alpha \left(\dfrac{\partial \psi}{\partial x}\, \mathbf{e}_x + \dfrac{V_{th}}{z_\alpha c_\alpha} \dfrac{\partial c_\alpha}{\partial x}\, \mathbf{e}_x + \dfrac{|z_\alpha| V_{th}}{z_\alpha c_p} \dfrac{\partial c_p}{\partial x} \mathbf{e}_x \right) & \forall (x,t) \in (\Omega_\alpha \times I_T) \end{cases} \tag{14}$$

As far as it regards the boundary conditions, all electrolytic ions α fulfill analogous boundary conditions. At the interface with the neuron, we enforce a Robin boundary condition on the flux density:

$$\mathbf{j}_\alpha \cdot \mathbf{n}_1 = -j_\alpha^{\text{tm}}(x) \quad \text{at } x = 0 \ \forall t \in I_T \tag{15}$$

This boundary condition describes the transmembrane coupling with the neuron, particularly accounting for the ionic motion across the neuron membrane driven by electric and diffusive gradients. The transmembrane molar flux density model adopted is that of Goldman-Hodgkin-Katz [17], Ch.17 , which defines j_α^{tm} for a generic ion α :

$$j_\alpha^{\text{tm}}(x) = -P_\alpha \left[c_\alpha(x,t)\ \mathcal{B}\left(z_\alpha \frac{V_m}{V_{th}} \right) - \bar{c}_\alpha^{N} \mathcal{B}\left(-z_\alpha \frac{V_m}{V_{th}} \right) \right] \tag{16}$$

where P_α represents the neuron membrane permeability to each ion α, $\bar{c}_\alpha^{N}$ is the fixed concentration of the ions inside the neuron and V_m is the membrane potential of the neuron, defined as the difference between the neuron and the extracellular electric potential ψ^{ex} , namely $V_m = \psi^N - \psi^{\text{ex}}$. In our model ψ^{ex} coincides with the cleft potential $\psi(x,t)$, with x= 0.

The equilibrium potential of the neuron ψ^N, is derived from the evaluation of the equilibrium membrane potential V_m^{eq}, computed with the Goldman formula [17], Ch.17,

$$V_m^{\text{eq}} = \psi^N - \psi^{\text{ex}} = V_{th} \ln \left(\frac{P_{K^+} c_{K^+}^{\text{bulk}} + P_{Na^+} c_{Na^+}^{\text{bulk}} + P_{Cl^-} \bar{c}_{Cl^-}^{N}}{P_{K^+} \bar{c}_{K^+}^{N} + P_{Na^+} \bar{c}_{Na^+}^{N} + P_{Cl^-} c_{Cl^-}^{\text{bulk}}} \right) \tag{17}$$

assuming $\psi^{\text{ex}} = 0$:

$$V_m^{\text{eq}} = \psi^N \tag{18}$$

$\mathcal{B}$ is the inverse of the Bernoulli function

$$\mathcal{B}(\Phi) := \frac{\Phi}{e^{\Phi} - 1} \tag{19}$$

which satisfies the following properties:

- $\mathcal{B}(\Phi) > 1 \quad \forall \Phi \in \mathbb{R}$
- $\mathcal{B}(0) = 1$
- $e^{\Phi}\mathcal{B}(\Phi) = \mathcal{B}(-\Phi) = \Phi + \mathcal{B}(\Phi)$

The transmembrane molar flux density j_{α}^{tm} is defined with a conventional direction of the particle current which flows from the neuron towards the extracellular space. In our model, we have the opposite perspective and this justifies the minus sign in eq. (20).

As far as it regards the behaviour of the ions at the extracellular endpoint x=W, we assume their concentrations to be given and equal to those of the bulk extracellular medium. This assumption is reasonable considering the reduced dimension of the NP compared to the surrounding biological medium, which far from the NP cannot be altered.

$$c_{\alpha} = c_{\alpha}^{\text{bulk}} \quad \text{at } x = W \;\; \forall t \in I_T \tag{20}$$

Here we do not enforce any boundary condition at x=R_1 and x=R_2 for the ions constituting the extracellular medium, since we are solving them across a continuum domain Ω_{α}

The superoxide

Besides the ions dissolved in the extracellular medium electrolyte, the superoxide O_2^- ion is of utmost importance in the characterization of the working principles of the retinal prosthesis. In particular, it can affect both the electric polarization of the NP and of the surrounding region, as well as induce a chemical effect due to its evolution into a ROS species, namely hydrogen peroxide. Unlike the other ions, the superoxide is produced at the electrochemically active interface of the NP and is available in solution at small equilibrium concentrations, of the order of 1 nM. Due to its ability to either recombine into hydrogen peroxide and to sustain an equilibrium condition concentration, we have introduced a bulk generation-recombination phenomenon.

The superoxide ion equation is solved in a piecewise function, first in Ω_1 and Ω_3 to account for the electrochemical effect of the NP and then in Ω_2^{bis}, assuming as interface conditions the previously calculated concentrations at R_1 and R_2. The continuity equation for the O_2^- reads:

$$\begin{cases} \dfrac{\partial c_{O_2^-}}{\partial t} + \nabla_x \cdot \mathbf{j}_{O_2^-} = \mathcal{G} - \mathcal{R} & \forall (x,t) \in (\Omega_1 \cup \Omega_2^{\text{bis}} \cup \Omega_3 \times I_T) \\ \mathbf{j}_{O_2^-} = \mu_{O_2^-} c_{O_2^-} \dfrac{\partial \psi}{\partial x}\, \mathbf{e}_x - D_{O_2^-} \dfrac{\partial c_{O_2^-}}{\partial x}\, \mathbf{e}_x & \forall (x,t) \in (\Omega_1 \cup \Omega_2^{\text{bis}} \cup \Omega_3 \times I_T) \end{cases} \tag{21}$$

Generation-recombination model In order to model the generation and recombination term of the O_2^- in the bulk of the electrolyte, we have chosen to utilize a net recombina-

tion/generation term with the following shape:

$$\mathcal{G} - \mathcal{R} = k_1 c_{O_2}^{eq} \left(1 - \frac{c_{O_2^-}}{c_{O_2^-}^{eq}}.\right) \tag{22}$$

The functional shape has been approximated from the rate equations of the following reactions:

$$\begin{aligned} O_2 + e^- &\xrightarrow{k_1} O_2^- \\ 2O_2^- + 2H^+ &\xrightarrow{k_2} H_2O_2 + O_2 \end{aligned} \tag{23}$$

We assume the generation of O_2^- in the bulk of the material to be secondary to the presence of molecular oxygen in solution, which, with a certain probability dissociates into O_2^-. This phenomenon is supposed to be the one that maintains an equilibrium concentration of the superoxide of no more than 1 nM. In competition with this phenomenon, we also observe the evolution of superoxide into hydrogen peroxide. This phenomenon in a biological environment may occur either spontaneously or favored by the superoxide dismutase enzyme [14]:

$$\frac{dc_{O_2^-}}{dt} = k_1 c_{O_2} - k_2 c_{H^+} c_{O_2^-} \tag{24}$$

The value of k_2 is assumed to be an averaged value between the rate of spontaneous and enzyme-driven dissociation, $k_2 = 8 \cdot 10^5$ $mM^{-1}s^{-1}$. In order to estimate the value of k_1 we have performed several approximations and modeling steps.

- $\frac{dc_{O_2^-}}{dt} = 0$: when the biological system is at equilibrium, the superoxide concentration can be considered as a constant value and its time evolution can be neglected. In this condition, we can obtain an expression for k_2 such as:

$$k_2 = \frac{k_1 c_{O_2}^{eq}}{c_{O_2^-}^{eq} c_{H^+}^{eq}} \tag{25}$$

- from eq. (25) and knowing $k_2 = 8 \cdot 10^5$ $mM^{-1}s^{-1}$, we can assign to k_1 the value of $3 \cdot 10^{-5}$ s^{-1}, assuming the ionic equilibrium concentration equal to $c_{O_2^-}^{eq} = 1$ nM, $c_{H^+}^{eq} = 10^{3-pH}$ mM, assuming a physiological pH of 7.4, and $c_{O_2}^{eq} = 1.04$ mM, derived from a partial pressure of oxygen in rats retinas of 20 mmHg, measured in Linsenmeier and Zhang [9].

- We assume in our time (and then also in space) domain of the model that the concentration of molecular oxygen and of hydrogen coincide with their equilibrium values $c_{O_2} := c_{O_2}^{eq}$ and $c_{H^+} := c_{H^+}^{eq}$.

Following this treatment, we can substitute the expression of eq. (25) into eq. (26) and obtain:

$$\frac{dc_{O_2^-}}{dt} = k_1 c_{O_2}^{eq} \left(1 - \frac{c_{O_2^-}}{c_{O_2^-}^{eq}}.\right) \tag{26}$$

This expression describes the time rate of change of the superoxide ion with respect to its equilibrium concentration.

Boundary and interface conditions At every time step, we enforce no-flux boundary conditions at both endpoints, namely:

$$\begin{aligned} \mathbf{j}_{O_2^-} \cdot \mathbf{n}_1 &= 0 \quad \text{at } x = 0 \quad \forall t \in I_T \\ \mathbf{j}_{O_2^-} \cdot \mathbf{n}_3 &= 0 \quad \text{at } x = W \quad \forall t \in I_T \end{aligned} \tag{27}$$

whereas at the interface we couple the superoxide interface production and recombination to the fluxes of electrons exiting the NP and to the surface recombination of holes:

$$\begin{aligned} \mathbf{j}_{O_2^-} \cdot \mathbf{n}_1 &= \frac{J_{REC}(x,t)}{F} - \frac{J_{MG}(x,t)}{F} \quad \text{at } x = R_1 \ \forall t \in I_T \\ \mathbf{j}_{O_2^-} \cdot \mathbf{n}_3 &= \frac{J_{REC}(x,t)}{F} - \frac{J_{MG}(x,t)}{F} \quad \text{at } x = R_2 \ \forall t \in I_T \end{aligned} \tag{28}$$

The hydrogen peroxide

The superoxide dynamic of eq. (23) predicts a reaction process leading towards the production of H_2O_2: hydrogen peroxide is an important reactive oxygen species (ROS) and a precise quantification of its dynamic and concentration may help shed light onto its possible role in the coupling with the neuron. The evaluation of hydrogen peroxide is performed solely in Ω_1, where its concentration is relevant due to the proximity with the biological environment. In order to provide this information with the model we have solved the following partial differential equation for $c_{H_2O_2}$:

$$\begin{cases} \dfrac{\partial c_{H_2O_2}}{\partial t} + \nabla_x \cdot \mathbf{j}_{H_2O_2} = \mathcal{G}(c_{O_2^-}) - \mathcal{R} & \forall (x,t) \in (\Omega_1 \times I_T) \\ \mathbf{j}_{H_2O_2} = -D_{H_2O_2} \dfrac{\partial c_{H_2O_2}}{\partial x} \, \mathbf{e}_x & \forall (x,t) \in (\Omega_1 \times I_T) \end{cases} \tag{29}$$

The drift term is neglected in the present transport equation since the molecule does not show up a net charge and, therefore, is not affected by the presence of an electric field. At the boundary of the cleft domain we suppose that the hydrogen peroxide cannot exit and we enforce homogeneous Neumann condition of the form:

$$\mathbf{j}_{H_2O_2} \cdot \mathbf{n}_1 = 0 \quad \text{at } x = 0, R_1 \ \forall t \in I_T \tag{30}$$

Generation-recombination model Analogously to what has been done for the generation and recombination term of $c_{O_2^-}$, we write the ordinary differential equation which describes the behaviour of $c_{H_2O_2}$ in time.

$$\frac{dc_{H_2O_2}}{dt} = k_1 \frac{c_{O_2}^{eq}}{c_{O_2^-}^{eq}} c_{O_2^-} - k_{hyd} c_{H_2O_2} \tag{31}$$

The hydrogen peroxide concentration appears therefore to be linearly dependent from the superoxide concentration $c_{O_2^-}$ through the coefficient k_{hyd}. An estimation of this coefficient is obtained with the following procedure:

- $\dfrac{dc_{H_2O_2}}{dt} = 0$: when the biological system is in equilibrium, the hydrogen peroxide concentration can be considered as a constant value and its time evolution can be ne-

glected. In this condition, we can obtain the expression for k_{hyd} such as:

$$k_{hyd} = \frac{k_1 c^{eq}_{O_2}}{c^{eq}_{H_2O_2}} \tag{32}$$

where k_1 has been determined in the previous paragraph and $c^{eq}_{H_2O_2} = 1\mu M$, an extracellular value which is at the inferior limit to be negligible or partially induce Oxidative Eustress [19].

- the time dependent model can be reasonably applied to every point $x \in \Omega_1$ and therefore we can write:

$$\mathcal{G}(c_{O_2^-}) - \mathcal{R} = k_1 \frac{c^{eq}_{O_2}}{c^{eq}_{O_2^-}} c_{O_2^-} - k_{hyd} c_{H_2O_2} \quad \forall (x,t) \in (\Omega_1 \times I_T) \tag{33}$$

Holes and electrons

The model for the P3HT material has been validated in the work Chiaravalli et al. [3] and is used as a milestone in building up all the new features of the system mathematical representation. The time dependent equations for holes and electrons are solved solely in Ω_2.

$$\begin{cases} q\dfrac{\partial p}{\partial t} + \nabla_x \cdot \mathbf{J}_p = q(\mathcal{G} - \mathcal{R}) & \forall (x,t) \in (\Omega_2 \times I_T) \\ \mathbf{J}_p = -q\mu_p p \dfrac{\partial \psi}{\partial x}\,\mathbf{e}_x - qD_p \dfrac{\partial p}{\partial x}\,\mathbf{e}_x & \forall (x,t) \in (\Omega_2 \times I_T) \end{cases} \tag{34}$$

$$\begin{cases} q\dfrac{\partial n}{\partial t} - \nabla_x \cdot \mathbf{J}_n = q(\mathcal{G} - \mathcal{R}) & \forall (x,t) \in (\Omega_2 \times I_T) \\ \mathbf{J}_n = -q\mu_n n \dfrac{\partial \psi}{\partial x}\,\mathbf{e}_x + qD_n \dfrac{\partial n}{\partial x}\,\mathbf{e}_x & \forall (x,t) \in (\Omega_2 \times I_T) \end{cases} \tag{35}$$

The generation and recombination terms have been characterized in details in [3]. The functional shape of J_{MG} and J_{REC} are reported in [6], and are proportional to the available concentration of O_2^-, being in the present model $c_{O_2^-} = c_{O_2^-}(x,t)$.

$$\begin{aligned} -\mathbf{J}_n \cdot \mathbf{n}_2 &= J_{MG}(x,t) \qquad \text{at } x = R_1, R_2 \quad \forall t \in I_T \\ \mathbf{J}_p \cdot \mathbf{n}_2 &= J_{REC}(x,t) \qquad \text{at } x = R_1, R_2 \quad \forall t \in I_T \end{aligned} \tag{36}$$

Electric field and potential

The Poisson equation is solved in all Ω by solving the following system of equations:

$$\nabla_X \cdot \mathbf{D} = \rho \qquad \rho = \begin{cases} q(p-n) & \forall (x,t) \in (\Omega_2 \times I_T) \\ q\left(\sum_\alpha z_\alpha c_\alpha N_{av} + z_{O_2^-} c_{O_2^-} N_{av}\right) & \forall (x,t) \in (\Omega_1 \cup \Omega_2^{bis} \cup \Omega_3 \times I_T) \end{cases} \tag{37}$$

The dielectric constant is also defined as a piecewise constant function:

$$\mathbf{D} = \varepsilon \mathbf{E} \qquad \varepsilon(\mathrm{x}) = \begin{cases} \varepsilon_{\mathrm{cl}} & \forall \mathrm{x} \in \Omega_1 \\ \varepsilon_{\mathrm{pol}} & \forall \mathrm{x} \in \Omega_2 \\ \varepsilon_{\mathrm{w}} & \forall \mathrm{x} \in \Omega_2^{\mathrm{bis}} \cup \Omega_3 \end{cases} \tag{38}$$

The Poisson equation is first solved across the domain $\Omega_{\mathrm{np}} := \{\Omega_1 \cup \Omega_2 \cup \Omega_3\}$, enforcing at the interface with Ω_2, at x=R_1^-,R_2^+, the conditions which describe the capacitive coupling with the NP:

$$\begin{aligned} \mathbf{D} \cdot \mathbf{n}_1 &= c_{\mathrm{NP}}(\psi(\mathrm{R}_1^-) - \psi(\mathrm{R}_1^+)) \quad \text{at } \mathrm{x} = \mathrm{R}_1 \ \forall \mathrm{t} \in \mathrm{I}_\mathrm{T} \\ \mathbf{D} \cdot \mathbf{n}_2 &= c_{\mathrm{NP}}(\psi(\mathrm{R}_1^+) - \psi(\mathrm{R}_1^-)) \quad \text{at } \mathrm{x} = \mathrm{R}_1 \ \forall \mathrm{t} \in \mathrm{I}_\mathrm{T} \\ \mathbf{D} \cdot \mathbf{n}_2 &= c_{\mathrm{NP}}(\psi(\mathrm{R}_2^-) - \psi(\mathrm{R}_2^+)) \quad \text{at } \mathrm{x} = \mathrm{R}_2 \ \forall \mathrm{t} \in \mathrm{I}_\mathrm{T} \\ \mathbf{D} \cdot \mathbf{n}_3 &= c_{\mathrm{NP}}(\psi(\mathrm{R}_2^+) - \psi(\mathrm{R}_2^-)) \quad \text{at } \mathrm{x} = \mathrm{R}_2 \ \forall \mathrm{t} \in \mathrm{I}_\mathrm{T} \end{aligned} \tag{39}$$

At the endpoints of the domain we have instead two different situations. At x= 0 the model experiences the interface with the neuron and the effect of the surface charge accumulated on the membrane. The surface charge can be equivalently represented with the formula $\sigma = c_s \Delta\psi$, where c_s is the specific capacitance [$\mathrm{F\,m^{-2}}$] and $\Delta\psi$ is the voltage difference across the membrane. In our model, the specific capacitance is that of the neuron cellular membrane $c_{\mathrm{m}}^{\mathrm{N}}$ and is multiplied by the potential difference across the membrane, ψ^{N} being the potential of the neuron:

$$\mathbf{D} \cdot \mathbf{n}_1 = c_{\mathrm{m}}^{\mathrm{N}}(\psi(x, \mathrm{t}) - \psi^{\mathrm{N}}) \quad \text{at } \mathrm{x} = 0 \quad \forall \mathrm{t} \in \mathrm{I}_\mathrm{T} \tag{40}$$

At x=W, instead, we again consider the bulk of the electrolyte to be an electro-neutral region, which acts as a ground for the whole system.

$$\psi = 0 \quad \text{at } \mathrm{x} = \mathrm{W} \quad \forall \mathrm{t} \in \mathrm{I}_\mathrm{T} \tag{41}$$

Once the potential is known across Ω_{np}, we recover the potential across Ω_2^{bis} by enforcing at x=R_1^+,R_2^- as Dirichlet boundary conditions the potential values calculated at x=R_1^- and at x=R_2^+ when solving the previous system of equations.

All the simulations reported in the following, unless differently specified, are performed assuming a physiological value of light intensity reaching the photoreceptors, namely 0.2 $\mathrm{W\,m^{-2}}$ [2], a radius of the NP of 150 nm and a cleft thickness of 30 nm (both in agreement with Maya-Vetencourt et al. [12]) . All the other parameters are reported in [3] or in the present table 1.

Table 1: Parameters assumed full bio-hybrid model.

Parameters	Units	Value	Source
I_0	$\mathrm{W\,m^{-2}}$	0.2	[2]
k_p	$\mathrm{m^4\,s^{-1}}$	$1 \cdot 10^{-30}$	assumed
k_t	$\mathrm{m^4\,s^{-1}}$	$1 \cdot 10^{-30}$	[16]
c_NP	$\mathrm{F\,m^{-2}}$	7.45	[20]
$c^\mathrm{bulk}_{\mathrm{Na^+}}$	mM	108	[13]
$c^\mathrm{bulk}_{\mathrm{Cl^-}}$	mM	118	[13]
$c^\mathrm{bulk}_{\mathrm{K^+}}$	mM	10	[13]
$\overline{c}^\mathrm{N}_{\mathrm{Na^+}}$	mM	5	adapted from [5]
$\overline{c}^\mathrm{N}_{\mathrm{Cl^-}}$	mM	8	adapted from [5]
$\overline{c}^\mathrm{N}_{\mathrm{K^+}}$	mM	110	adapted from [5]
$D_{\mathrm{Na^+}}$	$\mathrm{m^2 s^{-1}}$	$1.33 \cdot 10^{-9}$	[13]
$D_{\mathrm{Cl^-}}$	$\mathrm{m^2 s^{-1}}$	$2.03 \cdot 10^{-9}$	[13]
$D_{\mathrm{K^+}}$	$\mathrm{m^2 s^{-1}}$	$1.96 \cdot 10^{-9}$	[13]
$P_{\mathrm{Na^+}}$	$\mathrm{m s^{-1}}$	$6 \cdot 10^{-11}$	[4]
$P_{\mathrm{Cl^-}}$	$\mathrm{m s^{-1}}$	$1 \cdot 10^{-9}$	[4]
$P_{\mathrm{K^+}}$	$\mathrm{m s^{-1}}$	$4 \cdot 10^{-10}$	[4]
$D_{\mathrm{O_2^-}}$	$\mathrm{m^2 s^{-1}}$	$0.21 \cdot 10^{-9}$	[15]
c^N_m	$\mathrm{F\,m^{-2}}$	$9 \cdot 10^{-3}$	measured
ψ^N	mV	-58	computed with eq. (17)

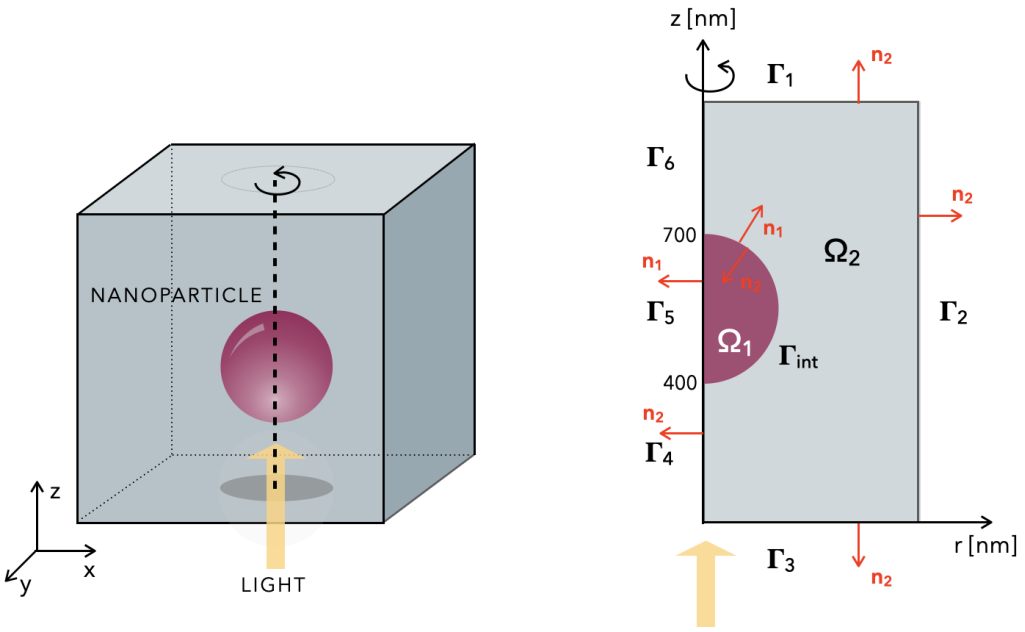

Figure 2: On the left we show a three-dimensional representation of a NP immersed in an external medium, which is approximated with a parallelepiped, in cartesian coordinated, with light impinging from the bottom. With dashed lines we highlight the axis of rotational symmetry exploited on the right to reduce the problem into a 2D axial symmetric geometry. This reduction does not affect the quality of the modeling, which is exactly equivalent to a 3D description, but allow a consistent saving in terms of computational effort.

The 2D-axial symmetric model

This section aims at describing the polarization and the charge reorganization inside a three-dimensional NP. The model accounts for a steady state description of the charge transport and of the interfacial mechanisms occurring at the NP, with a coupled solution of the Poisson equation, which is also solved into a neighbor environment. This version of the model aims at the study of the three-dimensional mechanisms occurring in the NP, not focusing onto the coupling mechanisms possibly occurring with the neuron.

The mathematical model

The present model comprises the drift diffusion model used to describe the NP physics generalized in a multi-dimensional domain. The surrounding environment is modeled as an empty space, characterized by a relative dielectric constant equal to ε_{cl}.

Neglecting electrolytic ions is a clearly a limitation of the model, which however mimics the dielectric proteinic contribution introduced the previous section: modeling the protein volume-filling contribution inside the transport equation of electrolytic ions effectively leads to a cleft depleted of ions. Apriori neglecting the presence of ions in the environment can therefore be seen as an effective simplified modeling of the **dielectric nature of the cleft**.

The geometrical framework of the problem is represented in fig. 2: due to the rotational symmetry of the real geometrical system (fig. 2-left), we can reduce a three-dimensional description into a 2D-axial symmetric ones, without losing generality nor accuracy in the

description, but gaining in terms of computational effort.

Spatial domain

Fig. 2 shows a three-dimensional schematic representation of the bio-hybrid system. This latter is composed of an NP (sphere, magenta color) and of a surrounding medium. The yellow arrow represents the external light input source, which in this model is supposed to arrive from the bottom of the domain. The rotational invariance of the system with respect to the z axis, in dashed lines in the three-dimensional picture on the left, allows us to reduce the 3D structure (in a Cartesian reference system) to the 2D axial symmetric (2DAS) structure depicted in the right panel of the figure, in r-z coordinate system. The computational domain of our model is the 2DAS region Ω, which is the union of the NP subdomain Ω_1 and of the subdomain Ω_2 of the surrounding medium. The boundary of Ω_1 is $\partial\Omega_1 = \Gamma_5 \cup \Gamma_{\text{int}}$, whereas the boundary of Ω_2 is $\partial\Omega_2 = \Gamma_1 \cup \Gamma_2 \cup \Gamma_3 \cup \Gamma_4 \cup \Gamma_6 \cup \Gamma_{\text{int}}$. We define the two dimensional axial symmetric set of coordinates as $\underline{\mathbf{x}} : \{r, z\}$.

Holes and electrons

The mathematical model for holes and electrons is a multi-dimensional version of the one reported in [3; 6]:

$$\begin{cases} \nabla_{\underline{x}} \cdot \mathbf{J}_{\text{p}} = q\,(\mathcal{G} - \mathcal{R}) & \forall \underline{\mathbf{x}} \in \Omega_1 \\ \mathbf{J}_{\text{p}} = -q\mu_{\text{p}} p \nabla_{\underline{x}} \psi - q D_{\text{p}} \nabla_{\underline{x}} p & \forall \underline{\mathbf{x}} \in \Omega_1 \end{cases} \tag{42}$$

$$\begin{cases} -\nabla_{\underline{x}} \cdot \mathbf{J}_{\text{n}} = q\,(\mathcal{G} - \mathcal{R}) & \forall \underline{\mathbf{x}} \in \Omega_1 \\ \mathbf{J}_{\text{n}} = -q\mu_{\text{n}} n \nabla_{\underline{x}} \psi + q D_{\text{n}} \nabla_{\underline{x}} n & \forall \underline{\mathbf{x}} \in \Omega_1 \end{cases} \tag{43}$$

To close the PDE system, we must enforce conditions along the whole $\partial\Omega_1$. Along the boundary coinciding with the symmetry axis Γ_5, we impose a homogeneous Neumann condition, respectful of the symmetric nature of the border. It reads:

$$\begin{aligned} \mathbf{J}_{\text{p}} \cdot \mathbf{n}_1 = 0 \qquad & \forall \underline{\mathbf{x}} \in \Gamma_5 \\ -\mathbf{J}_{\text{n}} \cdot \mathbf{n}_1 = 0 \qquad & \forall \underline{\mathbf{x}} \in \Gamma_5 \end{aligned} \tag{44}$$

Along the interface with the external environment, we impose the photo-cathodic boundary conditions :

$$\begin{aligned} \mathbf{J}_{\text{p}} \cdot \mathbf{n}_1 = \text{J}_{\text{REC}}(\underline{\mathbf{x}}) \quad & \forall \underline{\mathbf{x}} \in \Gamma_{\text{int}} \\ -\mathbf{J}_{\text{n}} \cdot \mathbf{n}_1 = \text{J}_{\text{MG}}(\underline{\mathbf{x}}) \quad & \forall \underline{\mathbf{x}} \in \Gamma_{\text{int}} \end{aligned} \tag{45}$$

Electric field and potential

The Poisson equation is solved in the whole Ω through the following system of equations:

$$\nabla_{\underline{x}} \cdot \mathbf{D} = \rho \qquad \rho = \begin{cases} q\,(p - n) & \forall \underline{\mathbf{x}} \in \Omega_1 \\ 0 & \forall \underline{\mathbf{x}} \in \Omega_2 \end{cases} \tag{46}$$

The dielectric constant is also defined as a piecewise constant function, which in Ω_2 may assume different values depending on the specific modeling conditions which will be specified for each simulation:

$$\mathbf{D} = \varepsilon \mathbf{E} \qquad \varepsilon = \begin{cases} \varepsilon_{\text{pol}} & \forall \underline{\mathbf{x}} \in \Omega_1 \\ \varepsilon_{\text{w,cl}} & \forall \underline{\mathbf{x}} \in \Omega_2 \end{cases} \tag{47}$$

To close the Poisson PDE, we must enforce the boundary and interface condition. Similarly to what has been done for holes, electrons and superoxide, we impose a homogeneous Neumann BC along the symmetry axis. The same condition is also imposed on Γ_1 and Γ_3, whereas the potential along Γ_2 is clamped to zero, assuming an electro-neutral environment far away from the NP:

$$\begin{aligned} \mathbf{D} \cdot \mathbf{n}_2 &= 0 \quad \forall \underline{\mathbf{x}} \in \Gamma_1 \cup \Gamma_3 \cup \Gamma_4 \cup \Gamma_6 \\ \mathbf{D} \cdot \mathbf{n}_1 &= 0 \quad \forall \underline{\mathbf{x}} \in \Gamma_5 \\ \psi(\underline{\mathbf{x}}) &= 0 \quad \forall \underline{\mathbf{x}} \in \Gamma_2 \end{aligned} \tag{48}$$

As far as it regards the interface with the NP, we suppose the occurrence of an accumulation of electrostatic charge, proportional to NP surface capacitance and to the potential difference across the interface. In the following we call ψ_1^{int} the electric potential at Γ_{int} defined in Ω_1, whereas ψ_2^{int} the electric potential at the same interface, but in Ω_2. Both ψ_1^{int} and ψ_2^{int} are function of the spatial set of coordinates $\underline{\mathbf{x}}$, such that $\psi_1^{\text{int}} = \psi_1^{\text{int}}(\underline{\mathbf{x}})$, $\psi_2^{\text{int}} = \psi_2^{\text{int}}(\underline{\mathbf{x}})$

$$\begin{aligned} \mathbf{D} \cdot \mathbf{n}_1 &= c_{\text{NP}} \left(\psi_1^{\text{int}}(\underline{\mathbf{x}}) - \psi_2^{\text{int}}(\underline{\mathbf{x}}) \right) \quad \forall \underline{\mathbf{x}} \in \Gamma_{\text{int}} \in \Omega_1 \\ \mathbf{D} \cdot \mathbf{n}_2 &= c_{\text{NP}} \left(\psi_2^{\text{int}}(\underline{\mathbf{x}}) - \psi_1^{\text{int}}(\underline{\mathbf{x}}) \right) \quad \forall \underline{\mathbf{x}} \in \Gamma_{\text{int}} \in \Omega_2 \end{aligned} \tag{49}$$

References

[1] Amin, M. and Küpper, J. [2020], 'Variations in proteins dielectric constants.', *Chem. Open* **9**(691-694s).

[2] Arnault, E., Barrau, C., Nanteau, C., Gondouin, P., Bigot, K., Viénot, F., Gutman, E., Fontaine, V., Villette, T., Cohen-Tannoudji, D., Sahel, J.-A. and Picaud, S. [2013], 'Phototoxic Action Spectrum on a Retinal Pigment Epithelium Model of Age-Related Macular Degeneration Exposed to Sunlight Normalized Conditions', *PLoS ONE* **8**(8), e71398.
URL: *https://dx.plos.org/10.1371/journal.pone.0071398*

[3] Chiaravalli, G., Manfredi, G., Sacco, R. and Lanzani, G. [2021], 'Photoelectrochemistry and Drift–Diffusion Simulations in a Polythiophene Film Interfaced with an Electrolyte', *ACS Applied Materials & Interfaces* **13**(30), 36595–36604.
URL: *https://pubs.acs.org/doi/10.1021/acsami.1c10158*

[4] Eaton, D. C., Russell, J. M. and Brown, A. M. [1975], 'Ionic permeabilities of anAplysia giant neuron', *The Journal of Membrane Biology* **21**(1), 353–374.
URL: *http://link.springer.com/10.1007/BF01941076*

[5] Fohlmeister, J. F., Cohen, E. and Newman, E. A. [2010], 'Mechanisms and distribution of ion channels in retinal ganglion cells: using temperature as an independent variable', *J. Neurophysiol.* **103**(3), 1357–74.

[6] Francia, S., Shmal, D., Di Marco, S., Chiaravalli, G., Maya-Vetencourt, J. F., Mantero, G., Michetti, C., Cupini, S., Manfredi, G., DiFrancesco, M. L., Rocchi, A., Perotto, S., Attanasio, M., Sacco, R., Bisti, S., Mete, M., Pertile, G., Lanzani, G., Colombo, E. and Benfenati, F. [2022], 'Light-induced charge generation in polymeric nanoparticles restores vision in advanced-stage retinitis pigmentosa rats', *Nature Communications* **13**(1), 3677.
URL: *https://www.nature.com/articles/s41467-022-31368-3*

[7] Khorobtykh, S., Havurinne, V., Mattila, H. and Tyystjarvi, E. [2020], 'Oxygen and ros in photosynthesis', *Plants* **9**(1), 91.

[8] Li, L., Li, C., Zhang, Z. and Alexov, E. [2013], 'On the dielectric "constant" of proteins: Smooth dielectric function for macromolecular modeling and its implementation in delphi', *J. Chem. Theory Comput.* **9**(2126-2136).

[9] Linsenmeier, R. A. and Zhang, H. F. [2017], 'Retinal oxygen: from animals to humans', *Prog Retin Eye Res* **58**, 115–151.

[10] Mailmberg, C. G. and Maryott, A. A. [1956], 'Dielectric constant of water from 0 ° to 100 ° c', *Journal of Research of the National Bureau of Standards* **56**(1), 2641.

[11] Maya-Vetencourt, J. F., Ghezzi, D., Antognazza, M. R., Colombo, E., Mete, M., Feyen, P., Desii, A., Buschiazzo, A., Di Paolo, M., Di Marco, S., Ticconi, F., Emionite, L., Shmal, D., Marini, C., Donelli, I., Freddi, G., Maccarone, R., Bisti, S., Sambuceti, G., Pertile, G., Lanzani, G. and Benfenati, F. [2017], 'A fully organic retinal prosthesis restores vision in a rat model of degenerative blindness', *Nature Materials* **16**(6), 681–689.
URL: *https://www.nature.com/articles/nmat4874*

[12] Maya-Vetencourt, J. F., Manfredi, G., Mete, M., Colombo, E., Bramini, M., Di Marco, S., Shmal, D., Mantero, G., Dipalo, M., Rocchi, A., DiFrancesco, M. L., Papaleo, E. D., Russo, A., Barsotti, J., Eleftheriou, C., Di Maria, F., Cossu, V., Piazza, F., Emionite, L., Ticconi, F., Marini, C., Sambuceti, G., Pertile, G., Lanzani, G. and Benfenati, F. [2020], 'Subretinally injected semiconducting polymer nanoparticles rescue vision in a rat model of retinal dystrophy', *Nature Nanotechnology* **15**(8), 698–708.
URL: *http://www.nature.com/articles/s41565-020-0696-3*

[13] Mori, Y. [2006], A Three-Dimensional Model of Cellular Electrical Activity, PhD thesis, New York University.

[14] Ohara, A. and Sayuri, M. [2011], *Principles of Free Radical Biomedicine*, Vol. 1, Nova Science Publisher.

[15] Reinsberg, P. H., Koellisch, A., Bawol, P. P. and Baltruschat, H. [2019], 'K-o2 electrochemistry: achieving highly reversible peroxide formation', *Phys Chem Chem Phys* **20**(21(8)), 4286–4294.

[16] Rudolph, M. and Ratcliff, E. L. [2017], 'Normal and inverted regimes of charge transfer controlled by density of states at polymer electrodes', *Nature Communications* **8**(1), 1048.
URL: *http://www.nature.com/articles/s41467-017-01264-2*

[17] Sacco, R., Guidoboni, G. and Mauri, A. G. [2019], *A Comprehensive Physically Based Approach to Modeling in Bioengineering and Life Sciences*, Academic Press.

[18] Schneider, M., Wagenpfahl, A., Deibel, C., Dyakonov, V., Schöll, A. and Reinert, F. [2014], 'Band bending at the P3HT/ITO interface studied by photoelectron spectroscopy', *Organic Electronics* **15**(7), 1552–1556.
URL: *https://linkinghub.elsevier.com/retrieve/pii/S1566119914000846*

[19] Sies, H. [2017], 'Hydrogen peroxide as a central redox signaling molecule in physiological oxidative stress: Oxidative eustress', *Redox Biology* **11**, 613–619.
URL: *https://linkinghub.elsevier.com/retrieve/pii/S2213231716303196*

[20] Tullii, G., Desii, A., Bossio, C., Bellani, S., Colombo, M., Martino, N., Antognazza, M. and Lanzani, G. [2017], 'Bimodal functioning of a mesoporous, light sensitive polymer/electrolyte interface', *Organic Electronics* **46**, 88–98.
URL: *https://linkinghub.elsevier.com/retrieve/pii/S1566119917301568*

[21] Verticchio Vercellin, A. C., Harris, A., Chiaravalli, G., Sacco, R., Siesky, B., Ciulla, T. and Guidoboni, G. [2021], 'Physics-based modeling of Age-related Macular Degeneration—A theoretical approach to quantify retinal and choroidal contributions to macular oxygenation', *Mathematical Biosciences* **339**, 108650.
URL: *https://linkinghub.elsevier.com/retrieve/pii/S0025556421000857*